A critical examination of force-extension relationship for freely jointed chain model

Hashem Moosavian[a], Tian Tang[a,*]

[a]*Department of Mechanical Engineering, University of Alberta, Edmonton, T6G 1H9, Alberta, Canada*

Abstract

The pioneering paper by (Kuhn, W., Grün, F., 1942. Kolloid-Zeitschrift 101, 248-271) provided a thorough understanding of the finite extensibility of the freely-jointed chain model in polymer science. In their work, the relative number of conformations are evaluated through the introduction of a non-Gaussian probability distribution for the free (subjected to zero force) chains. However, (Flory, P., 1969. Statistical Mechanics of Chain Molecules. Interscience Publishers) pointed out that this distribution does not truly describe the probability for the end-to-end vector of the chain. To tackle this issue, a corrected probability distribution was proposed and compared with the original form. Despite this improvement, numerous research studies still rely upon the original formulation of Kuhn and Grün, without being aware of Flory's correction. The present work attempts to clarify the fundamental difference between the two probabilities through recognition of the distinct underlying ensembles. Then, the influence of this correction is studied on the force-extension relationship of the individual chain, as well as on some well-known micromechanics-based network models. Finally, it is demonstrated that misuse of the probability distribution can lead to significant discrepancy in the force-extension relationship of a coil-rod chain, a model for the building

*Corresponding author
Email address: tian.tang@ualberta.ca (Tian Tang)

element of some biopolymer gels.

Keywords: Kuhn-Grün model, Freely-jointed chain model, Inverse Langevin function, Flory's correction, Statistical mechanics

1. Introduction

The statistical mechanics of the freely-jointed chain (FJC) model has a profound influence on the development of micromechanical insight into the macroscopic properties of polymers. Owing to its simplicity, the model has been widely applied in various branches of polymer science (Rubinstein and Colby, 2003). A FJC is assumed to consist of n consecutive rigid segments with identical length b (the Kuhn length) such that each segment is free to rotate in any direction. To determine the entropic elasticity of the chain, the primary objective of the FJC model is to evaluate the entropy of the system or equivalently the number of available conformations of the chain at any given end-to-end vector $\mathbf{r}$. Alternatively, the relative number of chain conformations can be related to the probability distribution of a "free" chain (not subjected to any forces) as a function of $\mathbf{r}$, i.e., $W_0(\mathbf{r})$. More precisely, $W_0(\mathbf{r})\mathrm{d}\mathbf{r}$ denotes the probability of finding one end of the free chain at volume element $\mathrm{d}\mathbf{r}$, while the other end is fixated at the origin. The simplest possible treatment is to postulate the Gaussian distribution for $W_0(\mathbf{r})$ (Kuhn, 1936). However, studies show that this distribution becomes increasingly inadequate as the end-to-end distance of the chain $|\mathbf{r}|$ approaches the fully extended length nb, especially with unrealistic nonzero values in the impermissible range $|\mathbf{r}| \geq nb$.

To overcome this difficulty, Kuhn and Grün (1942) propounded a more elaborate theory for the probability distribution of FJC with large n in the entire range of extension.

Their proposed non-Gaussian formulation led to a probability distribution involving the inverse Langevin function (Hereafter referred to as the inverse Langevin distribution), which recovers the Gaussian distribution for small end-to-end distance ($|\mathbf{r}| \to 0$). The pertinent force-extension relationship was also derived based on this probability distribution. Later, Treloar (1946) provided an exact form of the probability distribution for arbitrary values of n and end-to-end vector $\mathbf{r}$, at the cost of considerable sacrifice of simplicity. Accordingly, for practical purposes, the inverse Langevin distribution and the resulting force-extension relation are still in the spotlight of abundant research studies. They have contributed to different fields including the modelling of single chain behaviour (Volkenshteĭn et al., 1963; Treloar, 1975; Smith et al., 1992; Weiner, 2002; Rubinstein and Colby, 2003), its augmented versions accounting for extensibility (Smith et al., 1996; Fiasconaro and Falo, 2019; Buche et al., 2022) and coil-rod structure (Higgs and Ball, 1989), the development of macroscopic constitutive equations for single polymer networks (Wang and Guth, 1952; Treloar, 1954; Treloar et al., 1979; Arruda and Boyce, 1993; Wu and Van Der Giessen, 1993; Boyce and Arruda, 2000; Horgan and Saccomandi, 2002; Miehe et al., 2004; Bahrololoumi et al., 2020; Zhao et al., 2022), filled elastomers (Dargazany et al., 2014), double networks (Zhao, 2012; Liu et al., 2015; Zhong et al., 2020), nanocomposite hydrogels (Wang and Gao, 2016) and mechanochemically responsive polymers (Wang et al., 2015), as well as the study of photoelasticity (Treloar, 1954; Sun et al., 2021), damage and fracture phenomena (Lavoie et al., 2016; Mao et al., 2017; Vernerey et al., 2018; Lamont et al., 2021; Lei et al., 2021; Arunachala et al., 2021), to name but a few.

In contrast to the wide application of the model by Kuhn and Grün (1942), a noteworthy correction model by Flory (1969) has received scant attention. Specifically, Flory pointed out

that the proposed probability by Kuhn and Grün (1942) is established on the premise that the chain conformations have a given end-to-end displacement along an arbitrarily chosen direction rather than having a specific end-to-end vector $\mathbf{r}$. Subsequently, a modified version of the probability distribution $W_0(\mathbf{r})$ was provided. How should one understand the source of deviation between the original work by Kuhn and Grün and the modified version? What is the implication of this modification to the force-extension relationship for a single chain? How much will it impact the micromechanics-based constitutive models for polymer networks? The present study aims at answering these questions through a critical examination on the derivation of $W_0(\mathbf{r})$ and its influence on several network models.

For this purpose, in Section 2, different statistical ensembles are introduced to expound the difference between their associated probability distributions and clarify the force-extension relationship that can be derived from each ensemble. It is emphasized that both "force" and "extension" can have different meanings in different ensembles. Next, in Section 3, Flory's modification is implemented to the probability by Kuhn and Grün to determine the corrected force-extension relationship which is given by

$$\langle f_x \rangle_r = k_B T \frac{\beta}{b} + k_B T \left(\frac{1}{x} - \frac{\beta}{nb\left(1 - \beta^2 \mathrm{csch}^2 \beta\right)} \right). \tag{1}$$

In this equation, $\langle f_x \rangle_r$ is the average force applied at the ends of an FJC with a fixed end-to-end vector $\mathbf{r} = x\boldsymbol{i}$, k_B is the Boltzmann constant, and T is temperature. β is defined as

$$\beta = \mathscr{L}^{-1}\left(\frac{x}{nb}\right), \tag{2}$$

where $\mathscr{L}^{-1}(\cdots)$ is the inverse of the Langevin function $\mathscr{L}(\cdots)$ and $\mathscr{L}(s) = \coth(s) - 1/s$.

In comparison, the original force-extension relationship derived by Kuhn and Grün is

$$\langle f_x \rangle = \frac{k_B T}{b} \beta. \tag{3}$$

It will be shown that Eq. (3) predicts the average force on an FJC when its end-to-end displacement in x direction is fixed while the displacements along y and z directions can change freely. Fundamentally, $\langle f_x \rangle$ and $\langle f_x \rangle_r$ are different, but the former has been commonly used in the place of the latter. In Section 4, the preceding results are utilized to extract the stress-stretch curves for several network models under different loading conditions. Although results in Section 4 show that for large n the correction alters the results only slightly, Section 5 demonstrates that misuse of the probability distribution can cause large discrepancies, for instance, in the development of a force-extension relationship for a coil-rod structure.

2. FJC in different ensembles

In order to understand the nature of Flory's correction, it is beneficial to study several pertinent ensembles. In this section, different ensembles are described in detail, all with fixed temperature T and fixed number of Kuhn segment n.

2.1. Isothermal-isotension ensemble

Suppose that a chain is fixed at one end, while the other end is subjected to a force $\mathbf{f}$. The corresponding partition function is dependent on $\mathbf{f}$, temperature T, and n. For FJC, the exact form of the isothermal-isotension partition function is given by (Flory, 1969)

$$Q(\mathbf{f}, T, n) = Z_0 \left\{ \frac{\sinh\left[(k_B T)^{-1} b|\mathbf{f}|\right]}{(k_B T)^{-1} b|\mathbf{f}|} \right\}^n, \tag{4}$$

where $|\mathbf{f}|$ denotes the magnitude of vector $\mathbf{f}$. Z_0 refers to the same partition function in the absence of any external force $\mathbf{f}$ (i.e., for a free chain). The Gibbs free energy is calculated from $Q(\mathbf{f}, T, n)$ by

$$G(\mathbf{f}, T, n) = -k_B T \ln Q(\mathbf{f}, T, n). \tag{5}$$

Thus, the average of the chain's end-to-end vector is

$$\langle \mathbf{r} \rangle = -\frac{\partial G}{\partial \mathbf{f}} = k_B T \frac{\partial Q / \partial \mathbf{f}}{Q}. \tag{6}$$

Now, if the coordinate system is set up such that the x axis is aligned with the force direction (see Fig. 1a), then

$$|\mathbf{f}| = f_x, \tag{7}$$

$$f_y = f_z = 0. \tag{8}$$

The isothermal-isotension partition function (4) is rephrased as

$$Q(f_x, f_y = 0, f_z = 0, T, n) = Z_0 \left\{ \frac{\sinh\left[(k_B T)^{-1} b f_x\right]}{(k_B T)^{-1} b f_x} \right\}^n. \tag{9}$$

Substitution of Eq. (9) into (6) leads to

$$\langle x \rangle = nb \mathscr{L}\left(\frac{f_x b}{k_B T}\right), \tag{10}$$

and

$$\langle y \rangle = \langle z \rangle = 0, \tag{11}$$

since the partition function (9) is independent of f_y and f_z.

2.2. Canonical ensemble

Suppose that the chain ends are fixed at two points separated by the end-to-end vector $\mathbf{r}$. Different conformations of the chain constitute the canonical ensemble with fixed $\mathbf{r}$, T, and n. The Helmholtz free energy is related to the canonical partition function $Z(\mathbf{r}, T, n)$ by

$$\Psi(\mathbf{r}, T, n) = -k_B T \ln Z(\mathbf{r}, T, n). \tag{12}$$

The average force exerting on the chain ends is

$$\langle \mathbf{f} \rangle = \frac{\partial \Psi}{\partial \mathbf{r}} = -k_B T \frac{\partial Z / \partial \mathbf{r}}{Z}. \tag{13}$$

If the coordinate system is chosen such that the x axis is along the end-to-end vector (see Fig. 1b), then

$$|\mathbf{r}| = x, \tag{14}$$

$$y = z = 0. \tag{15}$$

Herein, the canonical partition function is written as $Z(x, y = 0, z = 0, T, n)$, and Eq. (13) is simplified to

$$\langle f_x \rangle_r = -k_B T \frac{\partial Z / \partial x}{Z}, \tag{16}$$

where $\langle f_x \rangle_r$ denotes the component of the average force along x direction. Since $Z(x, y = 0, z = 0, T, n)$ is independent of y and z,

$$\langle f_y \rangle_r = \langle f_z \rangle_r = 0, \tag{17}$$

and $\langle f_x \rangle_r$ is equal to the magnitude of $\langle \mathbf{f} \rangle$. The subscript r emphasizes this is the average force along the end-to-end vector of the chain.

To compute the canonical partition function, we note that $Z(\mathbf{r}, T, n)$ and $Q(\mathbf{f}, T, n)$ are related via the Laplace transform (Flory, 1969)

$$Q(\mathbf{f}, T, n) = \iiint Z(\mathbf{r}, T, n) \exp\left[(k_B T)^{-1} \mathbf{f} \cdot \mathbf{r}\right] \, \mathrm{d}\mathbf{r}. \tag{18}$$

In essence, $Q(\mathbf{f}, T, n)$ is determined by summing all possible $Z(\mathbf{r}, T, n)$ over different $\mathbf{r}$, weighted by the Boltzmann factor $\exp\left[(k_B T)^{-1} \mathbf{f} \cdot \mathbf{r}\right]$. By substituting Eq. (18) into Eq. (6), we obtain

$$\langle \mathbf{r} \rangle = \iiint \mathbf{r} W_{\mathbf{f}}(\mathbf{r}) \, \mathrm{d}\mathbf{r}, \tag{19}$$

where $W_{\mathbf{f}}(\mathbf{r})$ is the distribution function defined as

$$W_{\mathbf{f}}(\mathbf{r}) = \frac{Z(\mathbf{r}, T, n) \exp\left[(k_B T)^{-1} \mathbf{f} \cdot \mathbf{r}\right]}{\iiint Z(\mathbf{r}, T, n) \exp\left[(k_B T)^{-1} \mathbf{f} \cdot \mathbf{r}\right] \, \mathrm{d}\mathbf{r}}. \tag{20}$$

$W_{\mathbf{f}}(\mathbf{r})\mathrm{d}\mathbf{r}$ can be identified as the probability that, under the force $\mathbf{f}$, one end of the chain is at $\mathrm{d}\mathbf{r}$ while the other end is fixed at the origin. By setting $\mathbf{f} = \mathbf{0}$, one can obtain the probability density for one chain end to be at $\mathbf{r}$ in the absence of applied force, while the other end is fixed at the origin:

$$W_0(\mathbf{r}) = \frac{Z(\mathbf{r}, T, n)}{\iiint Z(\mathbf{r}, T, n) \, \mathrm{d}\mathbf{r}}. \tag{21}$$

For a chain subjected to zero force the probability $W_0(\mathbf{r})$ merely depends on the end-to-end distance r and not direction of $\mathbf{r}$; hence the vector $\mathbf{r}$ can be replaced by r in $W_0(\mathbf{r})$ and $Z(\mathbf{r}, T, n)$. Since $W_0(r)$ is proportional to $Z(r, T, n)$, it can replace $Z(r, T, n)$ in the calculation of $\langle f_x \rangle_r$ in Eq. (16), i.e.,

$$\langle f_x \rangle_r = -k_B T \, \frac{\partial W_0(x, y = 0, z = 0)/\partial x}{W_0(x, y = 0, z = 0)}. \tag{22}$$

Now we define another probability distribution as follows. Let $p_{\mathbf{f}}(x)\mathrm{d}x$ be the probability of finding one end of a chain under applied force $\mathbf{f}$ located in $\mathrm{d}x$ along $x-$direction, while the other end is fixed at the origin. Apparently,

$$p_{\mathbf{f}}(x) = \int_{y=-\infty}^{+\infty} \int_{z=-\infty}^{+\infty} W_{\mathbf{f}}(\mathbf{r})\, \mathrm{d}y\mathrm{d}z. \tag{23}$$

Substitution of (20) into (23) yields

$$p_{\mathbf{f}}(x) = \frac{\Pi(x, f_y, f_z, T, n)\exp\left[(k_B T)^{-1} f_x x\right]}{\int \Pi(x, f_y, f_z, T, n)\exp\left[(k_B T)^{-1} f_x x\right]\, \mathrm{d}x}, \tag{24}$$

where

$$\Pi(x, f_y, f_z, T, n) = \int_{y=-\infty}^{+\infty} \int_{z=-\infty}^{+\infty} Z(\mathbf{r}, T, n)\exp\left[(k_B T)^{-1} (f_y y + f_z z)\right] \mathrm{d}y\mathrm{d}z. \tag{25}$$

In the absence of applied force, the corresponding probability simplifies to

$$p_0(x) = \frac{\Pi(x, f_y = 0, f_z = 0, T, n)}{\int \Pi(x, f_y = 0, f_z = 0, T, n)\, \mathrm{d}x}. \tag{26}$$

Through analogy of the above result with (21), one can introduce a new ensemble which has $\Pi(x, f_y = 0, f_z = 0, T, n)$ as its partition function. We name this ensemble "semi-canonical ensemble" and explain it in detail below.

2.3. Semi-canonical ensemble

Consider an ensemble of chains with one end fixed at the origin. The other end is fixed along an arbitrarily chosen x axis, while its y and z positions are free to move. Moreover, the force applied at this end is zero along y and z directions. Evidently, this is neither the isothermal-isotension nor the canonical ensemble. The only difference between this new

ensemble and the isothermal-isotension ensemble is the specification of x rather than f_x (see Fig. 1c). It can be seen that

$$\langle y \rangle = \langle z \rangle = 0. \tag{27}$$

Similar to Eq. (16), the average of the applied force is given by

$$\langle f_x \rangle = -k_B T \, \frac{\partial \Pi(x, f_y = 0, f_z = 0, T, n)/\partial x}{\Pi(x, f_y = 0, f_z = 0, T, n)}. \tag{28}$$

By using Eq. (26), the average force can also be calculated from $p_0(x)$:

$$\langle f_x \rangle = -k_B T \, \frac{\partial p_0(x)/\partial x}{p_0(x)}. \tag{29}$$

3. FJC model of Kuhn and Grün

Kuhn and Grün (1942) determined the probability that the end-to-end vector of a FJC under no external force has a projection of x along an arbitrarily chosen x axis without constraints on y or z. This is precisely $p_0(x)\mathrm{d}x$ discussed in Section 2.3. The expression derived by Kuhn and Grün is

$$p_0(x) = c_0 \left(\frac{\sinh\beta}{\beta} \right)^n \exp\left[-\frac{\beta x}{b} \right], \tag{30}$$

where c_0 is the normalization factor and β is defined in Eq. (2). The detailed proof of Eq. (30) was provided in Kuhn and Grün (1942) as well as in Flory (1969). However, for the sake of self-containment, the derivation is given in Supplementary Material, Section S1. With the aid of (29), the associated force-extension relationship is obtained as given in Eq. (3). It should be emphasized that x here does not denote the end-to-end distance, instead it is the end-to-end displacement of the chain along x direction. Therefore, $\langle f_x \rangle$ represents the

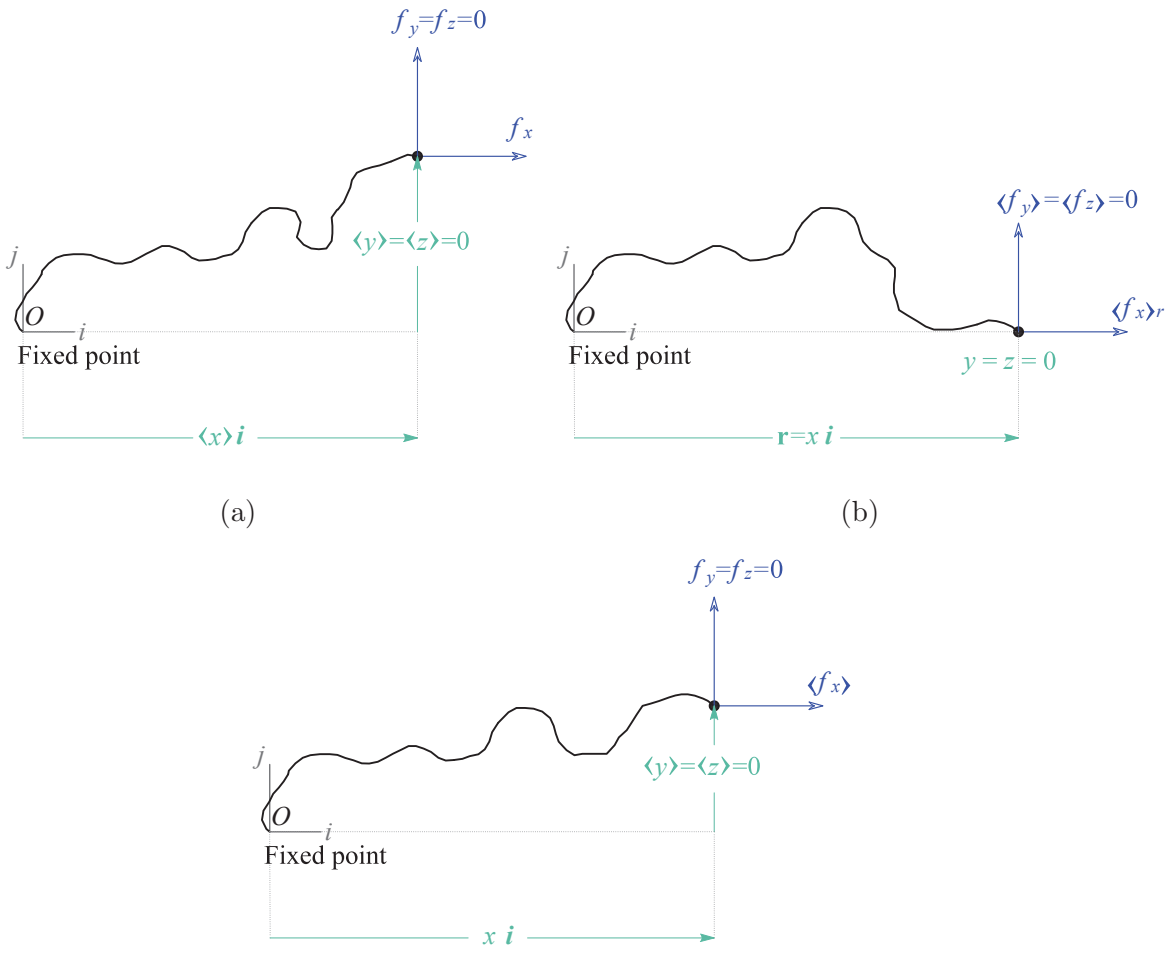

Figure 1: Different ensembles for a FJC with fixed number of Kuhn segments under constant temperature: (a) the isothermal-isotension ensemble in which the applied force is specified such that $f_y = f_z = 0$; (b) the canonical ensemble in which the components x, y, and z are fixed such that $y = z = 0$; (c) the semi-canonical ensemble in which different conformations occur with fixed x and fixed $f_y = f_z = 0$.

average force applied along the x axis in order to fix the end-to-end displacement along x while allowing the displacements along y and z directions to freely change. This average force is described in the framework of the partition function $\Pi(x, f_y = 0, f_z = 0, T, n)$ rather than $Z(x, y, z, T, n)$. However, in Kuhn and Grün (1942) an erroneous distribution $W^*(r)$ is derived by simply replacing x with r,

$$W^*(r) = c_0 \left(\frac{\sinh\beta^*}{\beta^*}\right)^n \exp\left[-\frac{\beta^* r}{b}\right], \tag{31}$$

where $\beta^* = \mathscr{L}^{-1}\left(\frac{r}{nb}\right)$.

When the FJC model is applied to evaluate the entropy of a polymer network, the probability relevant to the chains is $W_0(\mathbf{r}) = W_0(x = r, y = 0, z = 0)$ discussed in Section 2.2, and the relevant force-extension relationship is given by Eq. (22). However, (3) and the probability distribution (31) are used by many researchers unwittingly. $W_0(r)$ can be determined from $p_0(x)$ using the following relation (Treloar, 1946)

$$-\left(\frac{\mathrm{d}p_0(x)}{\mathrm{d}x}\right)_{x=r} = 2\pi r W_0(r). \tag{32}$$

The proof of the above relation is deferred to Supplementary Material, Section S2. By adopting the chain rule, the left-hand side of the above relation is rephrased as

$$\frac{\mathrm{d}p_0(x)}{\mathrm{d}x} = \left(\frac{\partial p_0(x)}{\partial\beta}\right)_x \frac{\mathrm{d}\beta}{\mathrm{d}x} + \left(\frac{\partial p_0(x)}{\partial x}\right)_\beta. \tag{33}$$

On the other hand the following identity holds for Eq. (30):

$$\left(\frac{\partial p_0(x)}{\partial\beta}\right)_x = c_0 n \left(\beta\sinh\beta\right)^n \exp\left[-\frac{\beta x}{b}\right]\left(\coth\beta - \frac{1}{\beta} - \frac{x}{nb}\right) = 0. \tag{34}$$

Now applying Eqs. (33) and (34) in Eq. (32) yields

$$W_0(r) = \frac{c_0\beta^*}{2\pi b r}\left(\frac{\sinh\beta^*}{\beta^*}\right)^n \exp\left[\frac{-\beta^* r}{b}\right], \tag{35}$$

which was mentioned in Flory (1969). Finally, substitution of Eq. (35) in (22) leads to Eq. (1). It should be noted that in Eq. (1) the second term is not singular as $x \to 0$, since $1 - \beta^2 \mathrm{csch}^2 \beta \sim \beta^2/3$ for small β and thus the second term converges to 0. The vast majority of the works using force-extension relationship of FJC have adopted $\langle f_x \rangle$ in (3) rather than $\langle f_x \rangle_r$ in (1). Unlike (3), $\langle f_x \rangle_r$ is not merely a function of x/nb, but also depends on n separately. Fig. 2 depicts the relative difference $\left| \dfrac{\langle f_x \rangle_r - \langle f_x \rangle}{\langle f_x \rangle_r} \right|$ vs. x/nb. Decreasing n as well as increasing x/nb give rise to larger discrepancies between the two formulations. On the other hand, for $n \geq 50$ the relative difference is less than 2%. The inset also compares the normalized forces $\langle f_x \rangle_r b/k_B T$ with $\langle f_x \rangle b/k_B T$ against x/nb for $n = 5$. Clearly, $\langle f_x \rangle b/k_B T$ overestimates the stiffness of the chain, especially near the fully extended state.

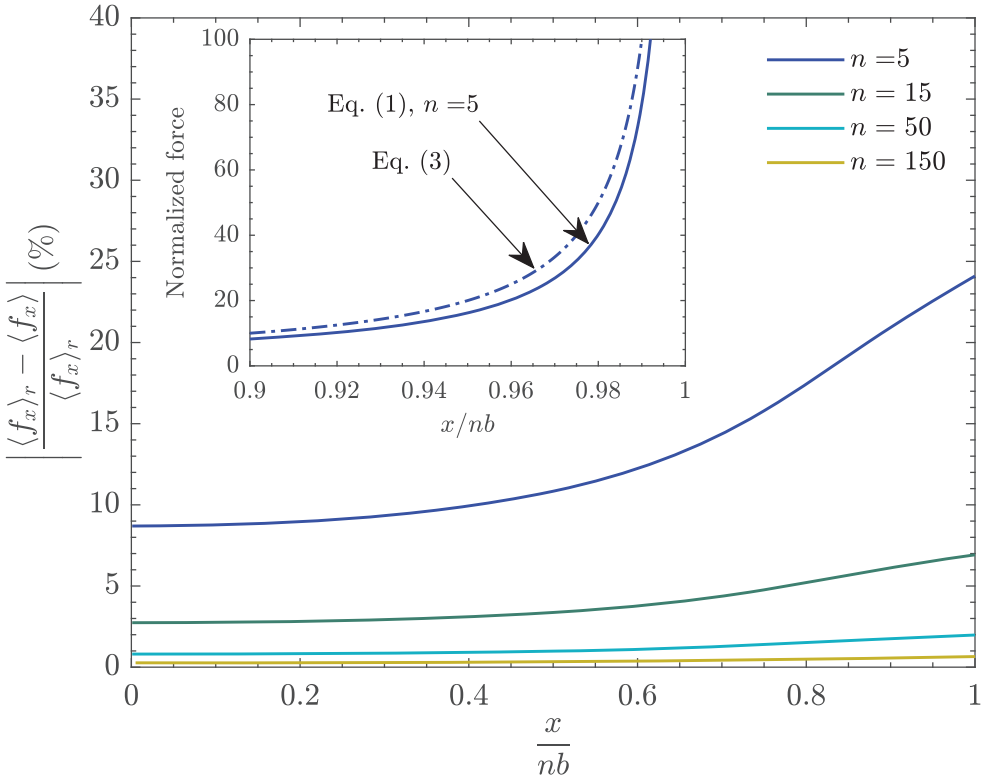

Figure 2: The relative difference between the average forces predicted by Eqs. (3) and (1) vs. the normalized end-to-end distance, for $n = 5$, 15, 50, and 150. The inset shows the normalized force vs. x/nb obtained from (3) and (1) for $n = 5$.

The above results show that increasing n causes the force-extension curves predicted from Eqs. (3) and (1) to converge. As $n \to \infty$, the statistical average of each property can be replaced by its thermodynamic value. In other words, the three pictures in Fig. 1 all correspond to the scenario where $y = z = 0$, $f_y = f_z = 0$, and f_x is applied to obtain x. Hence, the different ensembles can be employed interchangeably in the thermodynamic limit. Experimentally, single molecule stretching has been achieved by techniques such as atomic force microscopy (AFM). In the majority of the cases, the force-extension relationship given

by Eq. (3) or similar entropic elasticity based models is able to fit the experimental data up to a certain extension (Smith et al., 1992; Ghatak et al., 2000), beyond which entropic elasticity is insufficient and enthalpic elasticity needs to be considered. The good agreement with experimental data is due to the large length of the chain (i.e., large n), despite the application of erroneous Eq. (3). We should also point out that the corrected Eq. (1) suffers from the same limitation as Eq. (3) in the high-stretch regime, where adding extensibility is necessary to match experimentally measured force-extension relationship.

4. Implementation in macroscopic constitutive models

In the construction of macroscopic network models two factors are of cardinal importance: (a) the arrangement of the chains constituting the whole network structure; (b) the relation between force and end-to-end distance of the individual chains. For those models that use the FJC to account for entropic elasticity, the force-extension relationship of the chain plays an important role in the subsequent stress-stretch relation for the network. In accordance with the wide usage of the original inverse Langevin statistics, well-known models such as the three chain model (Wang and Guth, 1952), eight chain model (Arruda and Boyce, 1993), full network model (Wu and Van Der Giessen, 1993) and micro-sphere model (Miehe et al., 2004) utilized the $\langle f_x \rangle$-x relation in (3). In the current study, it is of interest to probe into the influence of using the $\langle f_x \rangle_r$-x relation (1) for deriving the macroscopic stress-stretch relation rather than Eq. (3). Herein, the full network and micro-sphere models (without any inclusion of tube-like constraints) are revisited with both (3) and (1); subsequently the pertinent results are compared for the equi-biaxial, uniaxial, and pure shear tests.

From macroscopic viewpoint, the Helmholtz free energy density (energy per unit reference

volume) Ψ is defined as a function of deformation gradient $\mathbf{F}$ and temperature T:

$$\Psi = \Psi_0 + \Psi(\mathbf{F}, T), \tag{36}$$

where Ψ_0 is the Helmholtz free energy density of the reference configuration. For incompressible materials, the Cauchy stress tensor is defined as

$$\boldsymbol{\sigma} = \frac{\partial \Psi}{\partial \mathbf{F}} \mathbf{F}^{\mathrm{T}} - P\mathbf{I}, \tag{37}$$

where $\mathbf{I}$ and P are the identity tensor and unknown hydro-static pressure, respectively. For the collection of chains forming a network, Ψ can be written as the summation of the Helmholtz free energy of the individual chains in a unit reference volume. Thus,

$$\Psi(\mathbf{F}, T) = \sum_{i=1}^{m} \psi_i(\lambda^{\mathbf{N}}), \tag{38}$$

where m is the number of chains in the unit reference volume, and $\lambda^{\mathbf{N}}$ refers to the micro-stretch of the chain initially oriented along unit vector $\mathbf{N}$. The micro-stretch is defined as the ratio of the current chain end-to-end distance to the corresponding value in the reference configuration, r_0. ψ_i is the Helmholtz free energy of the ith chain and can be related to $\langle f_x \rangle_r$ by

$$\psi_i(\lambda^{\mathbf{N}}) = \int_{r_0}^{r_0 \lambda^{\mathbf{N}}} \langle f_x \rangle_r \, \mathrm{d}x. \tag{39}$$

For the full network model (Wu and Van Der Giessen, 1993) the chains are assumed to be uniformly distributed in all directions in the reference configuration. Hence

$$\Psi(\mathbf{F}) = \frac{1}{4\pi} \iint_S m\psi(\lambda^{\mathbf{N}}) \mathrm{d}S, \tag{40}$$

where S denotes a spherical surface with unit radius in the reference configuration and $\psi = \psi_i$ given in (39). Insertion of the above relation in Eq. (37) yields

$$\boldsymbol{\sigma} + P\mathbf{I} = \frac{1}{4\pi} \iint_S m \frac{\partial \psi(\lambda^{\mathbf{N}})}{\partial \lambda^{\mathbf{N}}} \frac{\partial \lambda^{\mathbf{N}}}{\partial \mathbf{F}} \mathbf{F}^{\mathrm{T}} \mathrm{d}S. \tag{41}$$

By taking $r_0 = \sqrt{n}b$ as the end-to-end distance of the chain in the reference configuration, one can deduce that

$$\boldsymbol{\sigma} + P\mathbf{I} = \frac{1}{4\pi} \iint_S m\sqrt{n}b \langle f_x \rangle_r \Big|_{x=\sqrt{n}b\lambda^{\mathbf{N}}} \left(\frac{\partial \lambda^{\mathbf{N}}}{\partial \mathbf{F}} \mathbf{F}^{\mathrm{T}} \right) \mathrm{d}S. \tag{42}$$

To construct a proper relationship between the macroscopic deformation and micro-stretch, let us define the macro-stretch of a line element located along direction $\mathbf{N}$ in the reference configuration:

$$\bar{\lambda}^{\mathbf{N}} = \sqrt{\mathbf{N} \cdot \mathbf{F}^{\mathrm{T}} \mathbf{F} \mathbf{N}}. \tag{43}$$

For the affine network models, it is assumed that the micro-stretch of the chain is identical to the macro-stretch along the same direction $\mathbf{N}$, i.e.,

$$\lambda^{\mathbf{N}} = \bar{\lambda}^{\mathbf{N}}. \tag{44}$$

Fig. 3(a) and 3(b) illustrate this relationship. Now, applying Eqs. (43) and (44) in Eq. (42) leads to

$$\boldsymbol{\sigma} + P\mathbf{I} = \frac{1}{4\pi} \iint_S m\sqrt{n}b \langle f_x \rangle_r \Big|_{x=\sqrt{n}b\lambda^{\mathbf{N}}} \left(\bar{\lambda}^{\mathbf{N}}\right)^{-1} \left(\mathbf{N} \cdot \mathbf{F}^{\mathrm{T}} \mathbf{F} \mathbf{N}\right) \mathrm{d}S, \tag{45}$$

which completes the constitutive relation for the full network model.

Analogous to the previous treatment, a non-affine micro-sphere model can be developed in which (44) is no longer assumed. Instead, the following relation

$$\lambda^* = \left(\frac{1}{4\pi} \iint_S \left(\bar{\lambda}^{\mathbf{N}}\right)^p \mathrm{d}S \right)^{1/p} \tag{46}$$

is introduced to replace $\lambda^{\mathbf{N}}$, where p is an additional material parameter of the model. λ^* is essentially the stretch of the volume element averaged over different directions, as illustrated by Fig. 3(a) and 3(c). The free energy density of the network, $\Psi(\mathbf{F})$, can now be simplified to $m\psi(\lambda^*)$, where $\psi(\lambda^*) = \int_{r_0}^{r_0\lambda^*} \langle f_x \rangle_r \mathrm{d}x$. The Cauchy stress tensor is then given by

$$\boldsymbol{\sigma} + P\mathbf{I} = m\frac{\partial \psi(\lambda^*)}{\partial \lambda^*}\frac{\partial \lambda^*}{\partial \mathbf{F}}\mathbf{F}^{\mathrm{T}}. \tag{47}$$

Applying (46) in the above relation and assuming the end-to-end distance of $\sqrt{n}b$ in the reference configuration results in

$$\boldsymbol{\sigma} + P\mathbf{I} = \frac{1}{4\pi}\left(\lambda^*\right)^{1-p} m\sqrt{n}b\langle f_x \rangle_r\Big|_{x=\sqrt{n}b\lambda^*} \iint_S \left(\bar{\lambda}^{\mathbf{N}}\right)^{p-2}\left(\mathbf{N}\cdot\mathbf{F}^{\mathrm{T}}\mathbf{F}\mathbf{N}\right)\mathrm{d}S. \tag{48}$$

It should be emphasized that in the present formulation, the tube-like constraints on the individual chains are excluded for the sake of simplicity. In this case, the non-affine micro-sphere model with $p = 2$ collapses to the eight-chain model (Miehe et al., 2004).

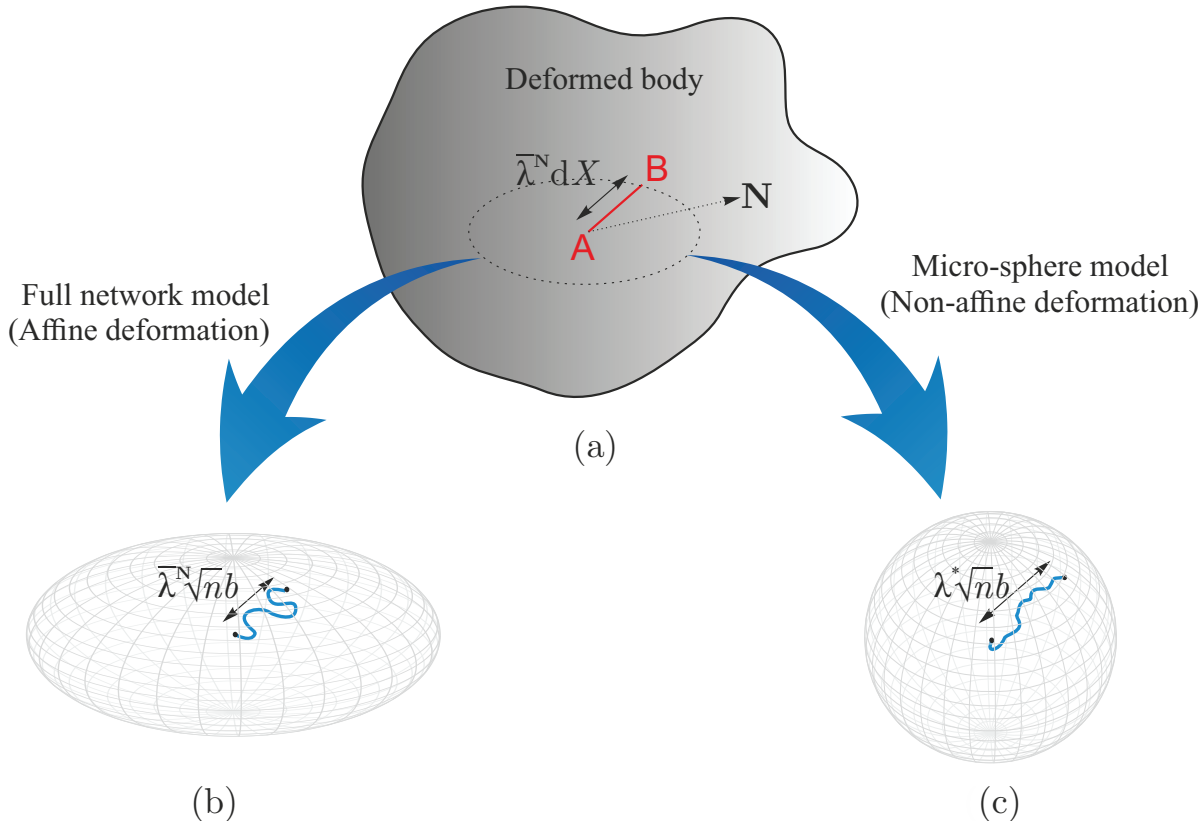

Figure 3: Schematic illustrations for the relationship between macroscopic stretch and microscopic chain extension in the full network and micro-sphere models. (a) Macroscopic deformation where a line element AB, originally oriented along $\mathbf{N}$ with length $\mathrm{d}X$, is deformed into $\bar{\lambda}^{\mathbf{N}}\mathrm{d}X$. (b) The full network model with affine deformation where the micro-stretch of the chain $\lambda^{\mathbf{N}}$ is assumed equal to the macro-stretch $\bar{\lambda}^{\mathbf{N}}$. The ellipsoid drawn indicates the dependence of $\lambda^{\mathbf{N}}$ on $\mathbf{N}$. (c) The micro-sphere model with non-affine deformation where the micro-stretch of the chain λ^{*} is obtained by an averaging process over different directions (indicated by the sphere drawn). In both (b) and (c) the initial end-to-end distance of the chain is considered as $\sqrt{n}b$.

Eqs. (45) and (48) connect the deformation gradient $\mathbf{F}$ to the Cauchy stress $\boldsymbol{\sigma}$; however, the selection of proper force-extension relation of the individual chains is a key factor in the

constitutive equations. By applying different relations such as those given in Eq. (3) or (1), different stress states in the macroscopic sample can be obtained for the same deformation. Fig. 4 displays the normalized Cauchy stress σ_{11}/G vs. the principal stretch λ_1 in equi-biaxial test, uniaxial test, and pure shear test for both affine (Eq. (45)) and non-affine models (Eq. (48)). $G = mk_BT$ is the shear modulus. In the non-affine model, the parameter p is set to 2 to recover the eight-chain model. The results are provided with different force-extension relationships (3) and (1) for $n = 10$ in order to depict the impact of Flory's correction at the macroscopic level. All integrations over the unit sphere were calculated numerically through the 21-point integration scheme of Bažant and Oh (1986).

By introducing the following dimensionless quantity as a measure of deviation

$$\eta = \frac{1}{\sqrt{G}(\hat{\lambda} - 1)} \int_1^{\hat{\lambda}} \sqrt{\left|\sigma_{11}^{(1)}(\lambda_1) - \sigma_{11}^{(2)}(\lambda_1)\right|} \mathrm{d}\lambda_1 \tag{49}$$

the total difference between the stress components $\sigma_{11}^{(1)}$ and $\sigma_{11}^{(2)}$ can be evaluated from the two different methods (superscripts (1) and (2) represent the use of Eqs. (3) and (1), respectively). The variable $\hat{\lambda}$ denotes the stretch at which the sample encounters chain locking without any further extension. All figures are drawn for extension λ_1 between 1 and $\hat{\lambda}$. Since the stress components are proportional to λ_1^{-1} as $\lambda_1 \to \hat{\lambda}$, the square root function is introduced to the integrand to ensure convergent integration for η. Based on η reported in the plots, for the full network model (Figs. 4a, 4c, 4e) the normalized stress in the equi-biaxial test possesses the maximum difference, while the differences for uniaxial and pure shear tests are smaller and approximately the same. In the eight-chain model (Figs. 4b, 4d, 4f), the equi-biaxial test has the minimum departure between the curves, while the uniaxial and pure shear tests exhibit larger deviations. Furthermore, comparison between the full network and eight-chain

models shows larger η for the latter. Hence, the eight-chain model is more sensitive to the correction of the force-extension relationship.

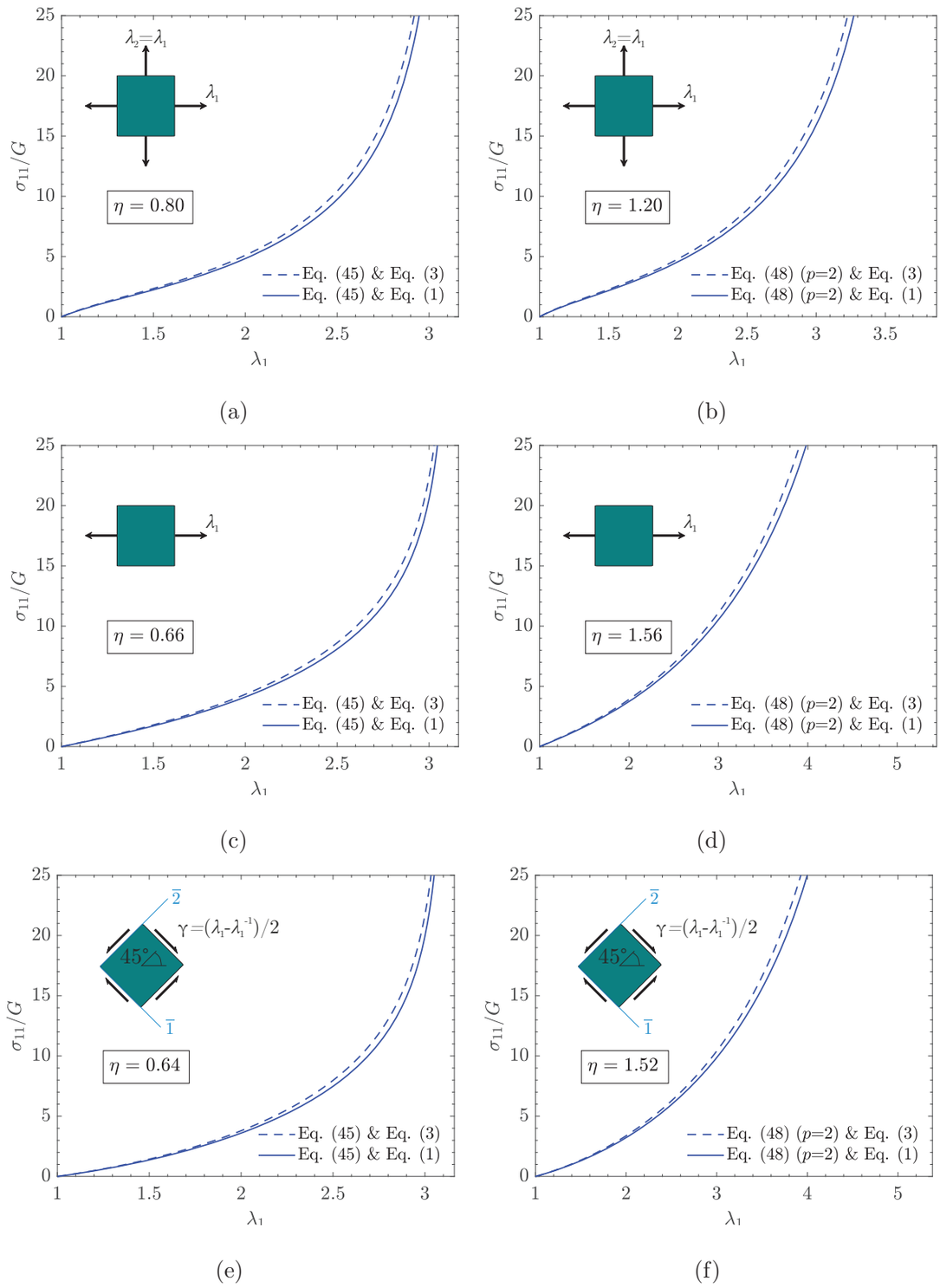

Figure 4: The normalized stress σ_{11}/G vs. λ_1 for equi-biaxial test in (a)-(b), uniaxial test in (c)-(d), and pure shear test in (e)-(f). (a), (c), (e) represent the affine (full network) model, while (b), (d), (f) display the non-affine micro-sphere model with $p = 2$. In all plots, λ_1 is the principal stretch in direction 1 (horizontal), and the other two principal directions are vertical, 2, and perpendicular to the page, 3. σ_{11} is the normal stress in direction 1. In pure shear, the deformation is given by $x_{\bar{1}} = \sqrt{1+\gamma^2}X_{\bar{1}} + \gamma X_{\bar{2}}$, $x_{\bar{2}} = \gamma X_{\bar{1}} + \sqrt{1+\gamma^2}X_{\bar{2}}$, and $x_{\bar{3}} = X_{\bar{3}}$ where x_i and X_i, $i = \bar{1}, \bar{2}, \bar{3}$ respectively denote the spatial and material coordinates. Directions $\bar{1}$ and $\bar{2}$ are shown in the insets of (e) and (f).